Separation of boron isotopes by gas phase membrane permeation of BF□3□
by Ronald Scott Herbst

A thesis submitted in partial fulfillment of the requirements for the degree of Master of Science in Chemical Engineering
Montana State University

Abstract:
The separation of boron isotopes by selective permeation of BF3 through a number of commercial and fabricated membranes was investigated.

The commercial films demonstrated little or no ability to fractionate boron isotopes, with calculated separation factors ranging between $\alpha = 1.000$ to $\alpha = 1.010$. The commercial films were studied at a pressure of 200 psig on the high pressure side of the membrane and at temperatures which gave a suitable permeation flux.

The fabricated membranes incorporated phenyl ether modifiers immobilized in a polyvinylidene fluoride support. With these fabricated membranes, enhanced selectivity for the mass 10 boron constituent of BF3 was observed. Separation factors of $\alpha = 1.020$ to $\alpha = 1.090$ were determined, depending on the ether incorporated in the membrane. Operating conditions were 200 psig on the upstream side of the membrane and a temperature of 120°C.

SEPARATION OF BORON ISOTOPES

BY GAS PHASE MEMBRANE

PERMEATION OF BF_3

by

Ronald Scott Herbst

A thesis submitted in partial fulfillment
of the requirements for the degree

of

Master of Science

in

Chemical Engineering

MONTANA STATE UNIVERSITY
Bozeman, Montana

June 1989

APPROVAL

of a thesis submitted by

Ronald Scott Herbst

This thesis has been read by each member of the thesis committee and has been found to be satisfactory regarding content, English usage, format, citations, bibliographic style, and consistency, and is ready for submission to the College of Graduate Studies.

5-16-89
Date

J P McCandless
Chairperson, Graduate Committee

Approved for the Major Department

5-16-89
Date

John T. Sears
Head, Major Department

Approved for the College of Graduate Studies

5/22/89
Date

Henry J Parsons
Graduate Dean

STATEMENT OF PERMISSION TO USE

In presenting this thesis in partial fulfillment of the requirements for a master's degree at Montana State University, I agree that the Library shall make it available to borrowers under rules of the Library. Brief quotations from this paper are allowable without special permission, provided that accurate acknowledgment of source is made.

Permission for extensive quotation from or reproduction of this thesis may be granted by my major professor, or in his absence, by the Dean of Libraries when, in the opinion of either, the proposed use of the material is for scholarly purposes. Any copying or use of the material in this thesis for financial gain shall not be allowed without my written permission.

Signature Ronald Scott Harold

Date May 16, 1989

ACKNOWLEDGEMENTS

The author wishes to thank Dr. Phil McCandless for his guidance, support and encouragement throughout the course of this investigation.

The author is gratefully indebted to Dr. Joe Sears, Chemistry Department, Montana State University, for his expert advice and help with the mass spectrometer.

Thanks are also extended to Jerry Paulson for his instrumental help in getting this project funded, and to Westinghouse Idaho Nuclear Company for financial support of this research.

Last, but not least, a special thanks goes to the author's wife, Danna Herbst, for her perseverance, encouragement and support during the course of this research.

TABLE OF CONTENTS

TABLE OF CONTENTS--Continued

LIST OF TABLES

LIST OF FIGURES

ABSTRACT

The separation of boron isotopes by selective permeation of BF_3 through a number of commercial and fabricated membranes was investigated.

The commercial films demonstrated little or no ability to fractionate boron isotopes, with calculated separation factors ranging between $\alpha = 1.000$ to $\alpha = 1.010$. The commercial films were studied at a pressure of 200 psig on the high pressure side of the membrane and at temperatures which gave a suitable permeation flux.

The fabricated membranes incorporated phenyl ether modifiers immobilized in a polyvinylidene fluoride support. With these fabricated membranes, enhanced selectivity for the mass 10 boron constituent of BF_3 was observed. Separation factors of $\alpha = 1.020$ to $\alpha = 1.090$ were determined, depending on the ether incorporated in the membrane. Operating conditions were 200 psig on the upstream side of the membrane and a temperature of 120°C.

INTRODUCTION

With man's capability to harness the energy of the atom and the subsequent advent of the "Atomic Age" came the need for new and different technologies. Prevalent was the need for an effective method for the containment or capture of neutrons, the relatively energetic subatomic particles generated in nuclear reactions. Among elements, boron absorbs neutrons readily. Interest in the separation of boron isotopes evolved largely from the contrasting difference in thermal neutron absorption cross-sections of these isotopes. Hence, there has been sustained interest in the separation of boron isotopes since shortly after the discovery of atomic fission.

Boron occurs naturally in two stable isotopic forms, one of mass 10 (^{10}B) and the other of mass 11 (^{11}B). Boron 10 constitutes 19.7 atom percent of natural boron and has a thermal neutron absorption cross-section of 3,837 barns [1]. Boron 11, which constitutes the remaining 80.3% of the total, has a thermal neutron absorption cross-section of only 0.005 barn [1]. The nuclear reaction:

$$^{10}_{5}B + ^{1}_{0}n \rightarrow ^{7}_{3}Li + ^{4}_{2}He + 2.4MeV$$

yields no secondary radiation effects since the lithium is stable and the alpha particles are easily stopped. Consequently, ^{10}B is particularly valuable as a neutron capture material. It is useful for neutron shielding, reactor control rods and as a neutron flux moderator or

neutron "poison." ^{10}B is 20 times more effective than lead and nearly 500 times more effective than concrete as a neutron shield for a given thickness [2, p. 1]. Based on this comparison, it is of little wonder that the nuclear industry thought the separation of boron isotopes to be imperative.

Historical Background

Prior to 1943, efforts to separate boron isotopes were confined primarily to thermal diffusion and mass spectroscopic techniques [3]. In 1943, during the early stages of the Manhattan Project, a group was established at Columbia University to study the separation of boron isotopes. Aside from one method based on thermal diffusion of BF_3, research was directed toward the distillation of various boron compounds, mainly BF_3-ether complexes. This work has been reported elsewhere in detail [3]. Isotopic distillation of the BF_3-dimethyl ether complex, $(CH_3)_2O$-BF_3, was selected for production-scale boron isotope separation. Accordingly, laboratory scale development was conducted at Columbia and pilot plant testing was performed by Standard Oil of Indiana from 1944 to 1946. In 1953, a production scale plant was constructed and operated by Hooker Electrochemical Company in Model City, New York. This plant was successfully operated from 1954-1958, with a total production of several hundred kilograms of 90-95% ^{10}B metal. This relatively low product output over a four year span testifies to the difficulties and problems associated with the isotopic distillation process. Complete details of these ventures are reported elsewhere [4,5].

In the early 1950's, the United States Atomic Energy Commission desired to have available separation methods of any or all of the isotopes of the lighter elements in the periodic table up through calcium. Partially in the wake of this desire and partly due to the need for a more efficient and less cumbersome method of boron isotope separation, Oak Ridge National Laboratory began evaluating potentially useful systems for the fractionation of boron isotopes in the mid-1950's. During the ten year course of that study, thirty molecular addition compounds of BF_3 were examined, ten of these in detail. Results of that study are reported elsewhere [2] and provide a great deal of insight into boron isotope chemistry.

Currently, Eagle-Pitcher Industries, Inc. operates the only boron isotope enrichment process in the United States. This facility, located in Quapaw, Oklahoma, still utilizes the isotopic distillation of BF_3 and the BF_3-dimethyl ether complex. Multiple distillations are effected in a series of 39 foot monel towers. The reported single-stage ideal separation factor in this distillation process is quite low at 1.016 [2]. The distillation is carried out at reduced pressure and recovery of the product is extremely difficult. Hence, the ^{10}B enriched product is relatively expensive. The most recent available figure for a 75% enriched ^{10}B sample is \$5.00 per gram of ^{10}B [6]. The major final product, ^{10}B enriched boric acid (H_3BO_3), is sold primarily to the Department of Energy for the weapons program.

Purpose and Scope of Investigation

This study was conceived for the sole purpose of investigating boron isotope separation by selective membrane permeation. The success of such an approach could ultimately spawn an improved, efficient and economical boron isotope separation method. Regardless of any ultimate success or failure, this study constitutes, to the best of the author's knowledge, the first recorded attempt to separate the isotopes of boron by selective permeation techniques.

Clearly, such a general study in so unexplored an area presents a number of avenues from which to approach the problem. The scope of this investigation was therefore limited to a few primary objectives. Consequently, this study was concerned with determining if and which commercially available polymeric films were non-reactive with and permeable to BF_3 gas. Potentially useful films were then examined to determine if any isotopic separation occurred during the permeation process. Thus, the commercial materials were studied to examine the possibility that boron isotopes exhibited different mass transport rates through these polymeric thin films. Preliminary results were also obtained for several thin films fabricated from polymer resins. These fabricated membranes were studied to deduce the plausibility of isotopic exchange reactions occurring interior to the membrane and resulting in enhanced separation during the permeation process.

THEORETICAL BACKGROUND

Chemical separation processes are generally based on differences in a physical property of the species to be separated. Membrane-based separations are no exception. The physical properties typically exploited in membrane separations are differences in solubilities and diffusion coefficients of a feed species in the membrane construction material. For the purposes of this discussion, a membrane will be defined as a thin, non-porous, polymeric barrier to dynamic flow which separates a volume into two distinct regions or compartments.

This study concerns binary component (two boron isotopes), gas phase permeation through non-porous polymeric membranes. Consequently, diffusional processes due to concentration or pressure gradients across the membrane are the primary mode of transport. The following discussion reflects these concerns by examining only gaseous permeation by a sorption-diffusion mechanism.

Nature of the Permeation Process

Permeation can be defined as the phenomenon in which chemical species are being transported across a membrane by diffusion. Thus, a membrane may be considered a region of discontinuity in a flow regime. As such, the flow regime may be characterized by five resistances to mass transport:

(1) Diffusion of the gas species from the high pressure bulk phase to the gas-membrane interface.

(2) Solution of the permeating species at the membrane surface.

(3) Diffusion of the species through the membrane.

(4) Desorption of the permeant species from the opposite membrane surface.

(5) Transport of the permeant from the membrane surface to the low pressure bulk phase.

The concentration profile across the entire permeation flow regime is represented graphically in Figure 1. The general shape of the concentration profile when all five of the above transport resistances are operative is represented in Figure 1(a).

In gas phase permeation, the diffusivity of the permeants through the membrane is generally quite low, typically 10^{-7} to 10^{-10} cm^2/sec [7, p. 509]. Gas phase diffusivities are generally orders of magnitude larger, typically 10^{-1} to 10^{-3} cm^2/sec [8, p. 3-256]. Consequently, perfect mixing throughout the bulk gaseous phases is a valid assumption and resistances (1) and (5) are usually negligible.

Further simplification of the transport mechanism is affected if partition equilibrium of the permeant species is maintained at the membrane interfaces. This assures that the free energy barriers opposing entry and release of the permeant species are negligible [9, p. 10]. Under these conditions, resistances (2) and (4) may also be neglected. The resulting steady state concentration profile for the case of a strictly diffusional process is represented in Figure 1(b).

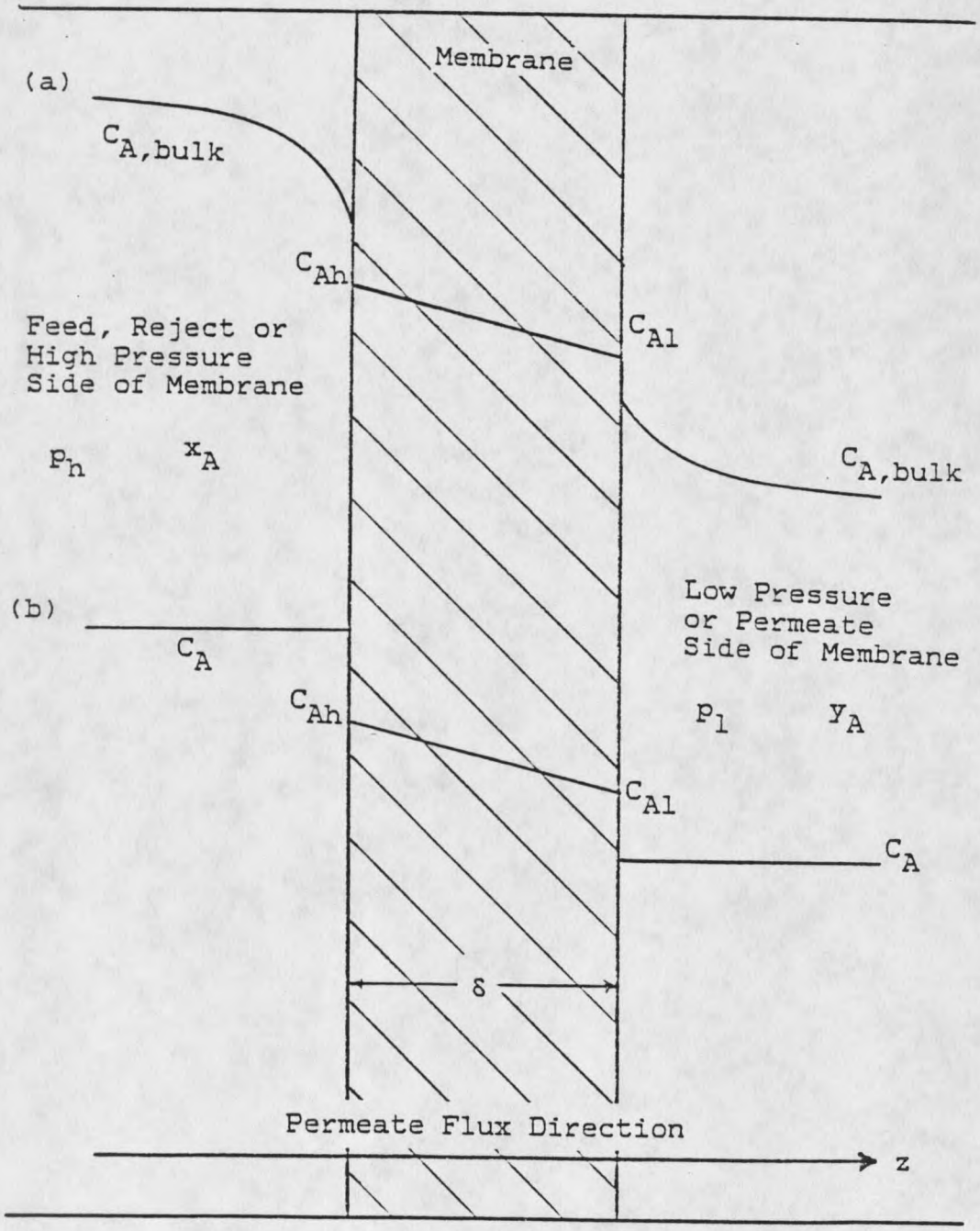

Figure 1. Concentration gradient through a gaseous permeation system. (a) With all transport resistances; (b) with only sorption/diffusion transport resistances.

In view of the above arguments, diffusion of the gaseous species through the membrane is the major transport resistance. Hence, gas phase permeation can generally be dealt with in terms of diffusion of a permeant species through a polymeric membrane. This simplified approach provides a very useful description for the nature of gas permeation.

Diffusive Transport Through a Membrane

Diffusion of gases through polymeric membranes greatly depends on whether the polymer is "glassy" or "rubbery." Rubbery polymers are characterized by a high degree of chain mobility, whereas in a glassy polymer chain mobility is greatly reduced. These two concepts are somewhat interrelated by the existence of a characteristic glass transition temperature, where the chain mobility and hence polymer state, is affected. The following discussion is restricted to gas diffusion through rubbery polymeric membranes.

The single component permeation flux of species A is adequately represented by Fick's first Law [10, p. 21]:

$$N_A = -D \frac{dC_A}{dz} \tag{1}$$

where D is the diffusion coefficient and C_A is the concentration of the permeating species in the membrane. Equation (1) reflects the following assumptions:

(1) The diffusivity is constant and independent of direction.

(2) Concentration is a function of only direction, thus whole derivatives are appropriate in equation (1).

The boundary conditions required for the solution of equation (1) are:

$$C_A = C_{Ah} \text{ at } z = 0$$

$$C_A = C_{Al} \text{ at } z = \delta$$

where δ is the membrane thickness. C_{Ah} and C_{Al} are the concentrations just inside the respective membrane interface. With these boundary conditions, equation (1) is readily integrated. Whence, upon rearrangement:

$$N_A = \frac{D_A}{\delta} (C_{Ah} - C_{Al}) \tag{2}$$

Equation (2) indicates that given membrane thickness, experimentally determined bulk concentrations and permeation flux, the overall diffusivity coefficient, D, can be calculated. The overall diffusivity obtained in this manner reflects not only the diffusivity of the permeant species, but the effect of the membrane on the permeation flux as well.

In the cases of gaseous systems, it is often convenient to express concentrations in terms of the partial pressures of the components. The concentrations and pressures of the permeant species in the membrane are generally quite low. Thus, it is appropriate to assume Henry's Law is a valid description of the permeant equilibrium at the membrane interfaces:

$$C_{Ah} = S_h p_h x_A \tag{3}$$

$$C_{Al} = S_l p_l y_A \tag{4}$$

The Henry's Law constant, S, is defined as the solubility of the gas species in the polymer. If the solubility coefficient is a function of

temperature only, and both sides of the membrane are maintained at the same temperature, then

$$S_h = S_l = S \tag{5}$$

Upon substitution of equations (3), (4) and (5), equation (2) can be rearranged to give the permeation flux as

$$N_A = \frac{SD}{\delta} (p_h x_A - p_l y_A) \tag{6}$$

This result indicates that the permeation flux is dependent upon the solubility and diffusivity of the permeant gas in the polymer membrane material. From this standpoint, the more soluble and/or diffusive components can be separated from a feed stream if the proper polymeric material is selected for membrane construction.

It is often convenient to define a mean permeability coefficient P* as

$$P^* \equiv SD \tag{7}$$

P* is often reported in the literature in units of barrers, where

$$1 \text{ barrer} = 10^{-10} \frac{\text{cm} \cdot \text{cm}^3(\text{STP})}{\text{cm}^2 \cdot \text{cmHg} \cdot \text{sec}}$$

This unit was named after R. M. Barrer, an early pioneer in membrane studies [11, p. 233].

Combination of equations (6) and (7) yields

$$N_A = \frac{P^*}{\delta} (p_h x_A - p_l y_A) \tag{8}$$

Equation (8) is the commonly encountered expression relating permeation flux to composition for gas phase permeation through rubbery polymers.

Temperature and Pressure Effects on Transport

For many gases above their critical temperatures, the Arrhenius type relations:

$$D = D_o \exp(-E_D/RT) \tag{9}$$

$$S = S_o \exp(-\Delta H_s/RT) \tag{10}$$

provide valid descriptions of the temperature effects on the diffusivity and solubility coefficients D and S, respectively [8, p. 15-17]. Increased temperatures therefore cause a corresponding exponential increase in the permeability coefficient defined by equation (7). Thus, according to equation (8), increased temperatures cause a corresponding increase in permeation flux.

Equation (2) was founded on the basis that a concentration gradient was the driving force for mass transport. For dilute gaseous systems, pressure is related to concentration through Henry's Law, equations (3) and (4). Thus, the permeation flux through a membrane is generally increased by increasing the pressure drop across the film.

Binary Component Permeation: The Separation Factor

It is often convenient to express equation (8) in terms of the molar flow rate of permeate, L:

$$L = \frac{A\, P_A^m}{\delta} \left(p_h x_A - p_l y_A\right) \tag{11}$$

Equation (11) was obtained by multiplication of equation (8) by the area perpendicular to the direction of flux, A, and the molar density. Hence P^m is the molar permeability of the species in the polymer.

For a binary component permeation process where species A and B are permeating simultaneously and non-interactively through the film, the following relationships hold:

$$y_A L = \frac{A\, P_A^m}{\delta} \quad (p_h x_A - p_l y_A) \tag{12}$$

$$(1-y_A)\, L = \frac{A\, P_B^m}{\delta} \quad [p_h(1-x_A) - p_l(1-y_A)] \tag{13}$$

Equations (12) and (13) are obtained by combination of binary component material balances with equation (11). Taking the ratio of equations (12) to (13) and cancelling like terms, the following relationship is obtained:

$$\frac{y_A}{(1-y_A)} = \frac{P_A^m}{P_B^m} \frac{[p_h x_A - p_l y_A]}{[p_h(1-x_A) - p_l(1-y_A)]} \tag{14}$$

Further simplification of (14) is effected by defining an overall separation factor α, and the pressure ratio p_r such that

$$\alpha \equiv \frac{y_A\,(1 - x_A)}{x_A\,(1 - y_A)} \tag{15}$$

$$p_r = p_l \,/\, p_h \tag{16}$$

Combination of equations (14), (15) and (16) with appropriate rearrangement yields the following relationship:

$$\alpha = \frac{P_A^m}{P_B^m} \quad \frac{(1 - x_A)/(1 - y_A)}{[(1-x_A)/(1-y_A)] + P_r\,[(P_A^m/P_B^m)-1]} \tag{17}$$

The overall separation factor, α, defined by equation (15) is a convenient measure of the degree of separation through a membrane. Equation (17) indicates α depends only on the ratio of the molar permeabilities, the reject mole fraction (x_A), the permeate mole fraction (y_A) and the pressure ratio across the membrane.

The ratio of permeabilities is defined as the ideal separation factor, α^*:

$$\alpha^* = P_A^m / P_B^m \tag{18}$$

The ideal separation factor depends only on temperature and the nature of the gas-membrane system. In gas phase permeation, the pressure ratio across the membrane is generally quite small, $p_r \ll 1$. Equation (17) indicates that as $P_r \to 0$, the overall separation factor reduces to the ideal separation factor ($\alpha = \alpha^*$).

In this study, the analysis of a successful separation was determined by equation (15). The steady state mole fractions of ^{10}B were determined in the reject and permeate streams for each tested membrane. The overall separation factor, α, was then calculated by equation (15). A membrane exhibiting an overall separation factor significantly greater than unity ($\alpha > 1$) could be potentially useful in a permeation technique for boron isotope fractionation.

Complex Transport

Due to the similarities in the chemical and physical properties of the boron isotopes, fractionation based on a strict sorption/diffusion permeation mechanism may not be plausible. However, it may be possible to enhance the selectivity of a polymeric film for boron isotope separation by incorporating a chemical agent which selectively interacts with one of the isotopes. In this research, several fabricated membranes were prepared in this laboratory to explore such a mechanism, defined as complex transport.

Complex transport results through a mechanism where a chemical reagent or carrier incorporated in the membrane reacts reversibly with a species in the feed mixture. The reaction product or chemical complex preferentially captures and transports one species across the membrane. Thus, the carrier must undergo a reversible complexation reaction with one species in the permeate selectively with respect to the other permeate components.

The idea of carrier mediated transport for the membrane separation of the boron isotopes evolved largely from the review of literature pertinent to the isotopic distillation process [2,3]. This process involved the chemical fractionation of boron isotopes between BF_3 gas and liquid molecular addition compounds or complexes of BF_3. Thus, the isotopic distillation was effected by passage of BF_3 gas flowing counter

currently to the liquid complex through a packed column. The distillation process is represented by the equilibrium reaction:

$$^{10}BF_{3(g)} + {}^{11}BF_3 \cdot complex_{(1)} \overset{\rightarrow}{\leftarrow} {}^{11}BF_{3(g)} + {}^{10}BF_3 \cdot complex_{(1)} \qquad (19)$$

The ^{10}B therefore concentrates in the descending liquid phase while the ^{11}B is concentrated in the upflowing vapor phase.

A number of BF_3 complexes were studied or screened by previous researchers for potential use in the isotopic distillation scheme [2]. Among the more potentially useful candidates for this system were the BF_3 complexes formed from the phenyl ethers: anisole ($C_6H_5OCH_3$), phenetole ($C_6H_5OC_2H_5$) and diphenyl ether ($C_6H_5OC_6H_5$). Consequently, these phenyl ethers were selected as carriers for the preliminary studies of complex membrane transport.

In the membranes fabricated for this study, the liquid phenyl ether or BF_3-ether complex was immobilized in a polyvinylidene fluoride (PVDF) membrane. The theory behind these fixed-site carrier, complex transport membranes was that the isotopic exchange reaction as given by equation (19) would occur within the membrane, a thermodynamic reaction equilibrium would be established throughout the film and thereby selectively transport the ^{10}B constituent of the feed across the membrane.

The ethers were effectively immobilized in the interstices of the PVDF lattice, or perhaps even covalently bonded to the lattice. Thus, the carrier ether was thought to occupy fixed sites in the membrane. The reversible complexation reaction was then envisioned as occurring continuously throughout the thickness of the thin film.

Theoretically, a purely diffusive flux of both isotopic constituents of BF_3 would exist through the PVDF lattice of the membrane. The fixed site carrier would provide an alternative route for the transport of $^{10}BF_3$. Hence, the mass 10 boron trifluoride molecules could effectively "jump" between carrier sites. This mechanism would result in enhancement of the $^{10}BF_3$ transport and an isotopic enrichment in the permeate stream. Under these conditions, the separation factor, α, was determined as given by equation (15):

$$\alpha = \frac{y_A\,(1-x_A)}{x_A\,(1-y_A)} \qquad (15)$$

Note that the complex transport mechanism is not necessarily restricted to enhanced $^{10}BF_3$ permeation. With the ether carriers, ^{10}B selectivity is the expected or postulated result. Other compounds, when used as carriers, could just as well show ^{11}B selectivity by the same mechanism. The overall separation factors for the two components of a binary system are related by:

$$\alpha\,(^{10}B) = \frac{1}{\alpha\,(^{11}B)} \qquad (20)$$

The relationship shown in equation (20) merely assures that the reported separation factors are greater than unity ($\alpha>1$), which is the accepted convention.

EXPERIMENTAL MATERIALS, EQUIPMENT AND PROCEDURES

Reagents and Materials

Boron trifluoride, BF_3, sometimes referred to as boron fluoride, was the selected feed gas for the boron isotope separation studies. A cylinder containing five pounds of this material at 1300 psig was obtained from the Matheson Gas Company, Inc. The BF_3 gas was of chemical purity (c.p.) grade, with a minimum reported purity of 99.5% BF_3. This material was used directly as feed stock for all permeation experiments with no attempt at further purification.

A cylinder of helium was obtained from the Alphagaz Company. This material was of ultra high purity (UHP) grade, with a minimum reported purity of 99.999% helium. The helium was used primarily to purge the experimental system prior to each permeation test. Such a high degree of purity was required by the mass spectral analysis procedure, since lesser purity helium was found to contain enough residual air to be detected by the mass spectrometer.

Polyvinylidene fluoride (PVDF) resin (Kynar®), Grade 301, was obtained from the Pennwalt Corp., Philadelphia, PA. This material was utilized as the polymer base in a number of "fabricated" membranes manufactured in this laboratory. The manufacturer lists the chemical structure of the PVDF resin as $(-CH_2-CF_2-)_n$.

Dimethyl formamide (DMF, $HCON(CH_3)_2$), reagent grade, was obtained from Baker Chemical Co., Phillipsburg, PA. This material was used as the solvent for the PVDF resin.

Anisole (C_6H_5-O-CH_3), phenetole (C_6H_5-O-C_2H_5), and diphenyl ether (C_6H_5-O-C_6H_5) were all obtained from the Aldrich Chemical Co., Milwaukee, WI, in I.R. grade purity. These phenyl ethers were used as "modifiers" or additives in the PVDF membranes.

A number of commercially available polymeric plastics were used as membranes. In the list of these materials that follows, all films were manufactured by E. I. Dupont De Nemours Co., Inc., Wilmington, DE, unless otherwise noted.

Teflon® (FEP) fluorocarbon film, type 200A, obtained in 2 mil thickness.

Tedlar® polyvinylfluoride (PVF) film.

Cellulose acetate, type 100CA43, 2 mil thickness.

Mylar® polyester film, type S, 50 gauge (0.5 mil thickness)

Kapton® polyimide film, type 100H, 1 mil thickness.

Cellophane type PD150 film, 1.3 mil thickness.

Clysar P® polyolefin (polypropylene) type P-1A3 film, 0.85 mil thickness.

Polyethylene type A, 1.25 mil thickness.

Polyethersulfone (PES) film, manufactured by Westlake Plastics Co., Lenni, PA.

Polysulfone, 5 mil thickness, obtained from Union Carbide.

Capran® 77C nylon film, manufactured by Allied Chemical Co., 1 mil thickness.

Trycite® polystyrene film, 1 mil thickness, Dow Chemical, Midland, MI.

Saran® polyvinylidene chloride, polyvinyl chloride copolymer, Dow Chemical, Midland, MI.

Equipment and Apparatus

The experimental permeation system is shown schematically in Figure 2. The major system components include: (1) permeation cell; (2) feed supply; (3) sample capture and flow measurement equipment; (4) constant temperature enclosure; and (5) helium purge gas system. The entire experimental apparatus was assembled in a fume hood to prevent accidental human exposure to the BF_3 gas. The major system components are described separately below.

Permeation Cell

The "heart" of the experimental system is the permeation cell. This device supports and houses the thin polymeric membrane and separates the experimental system into regions of high and low pressure. An exploded schematic indicating the permeation cell construction arrangement is shown in Figure 3. The cell body consists of two stainless steel flanges, 6.5 centimeters in diameter, which are held together by a large compression nut. A porous monel or stainless steel disc fits snugly into the cavity of the low pressure flange. This disc provides the necessary membrane support while allowing unrestricted flow of the permeant gas.

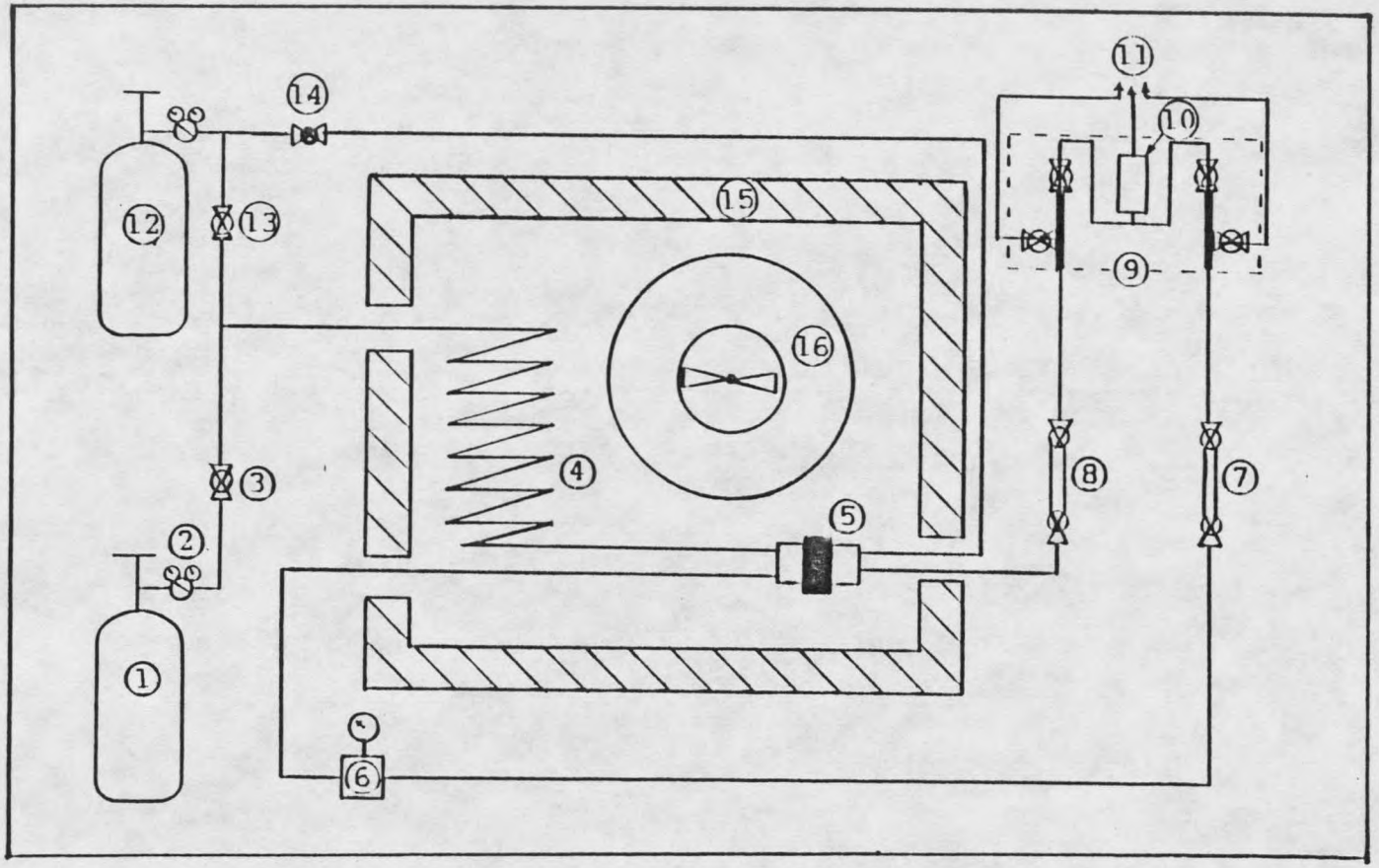

Figure 2. Permeation equipment diagram. (1) Feed gas, (2) pressure regulator, (3) feed control valve, (4) heat exchanger coil, (5) permeation cell, (6) back pressure regulator, (7) reject sample capture reservoir, (8) permeate sample capture reservoir, (9) flow measurement manifold, (10) flow transducer, (11) vent, (12) purge gas, (13) high pressure purge control valve, (14) permeate purge control needle valve, (15) constant temperature enclosure, (16) fan and heater assembly.

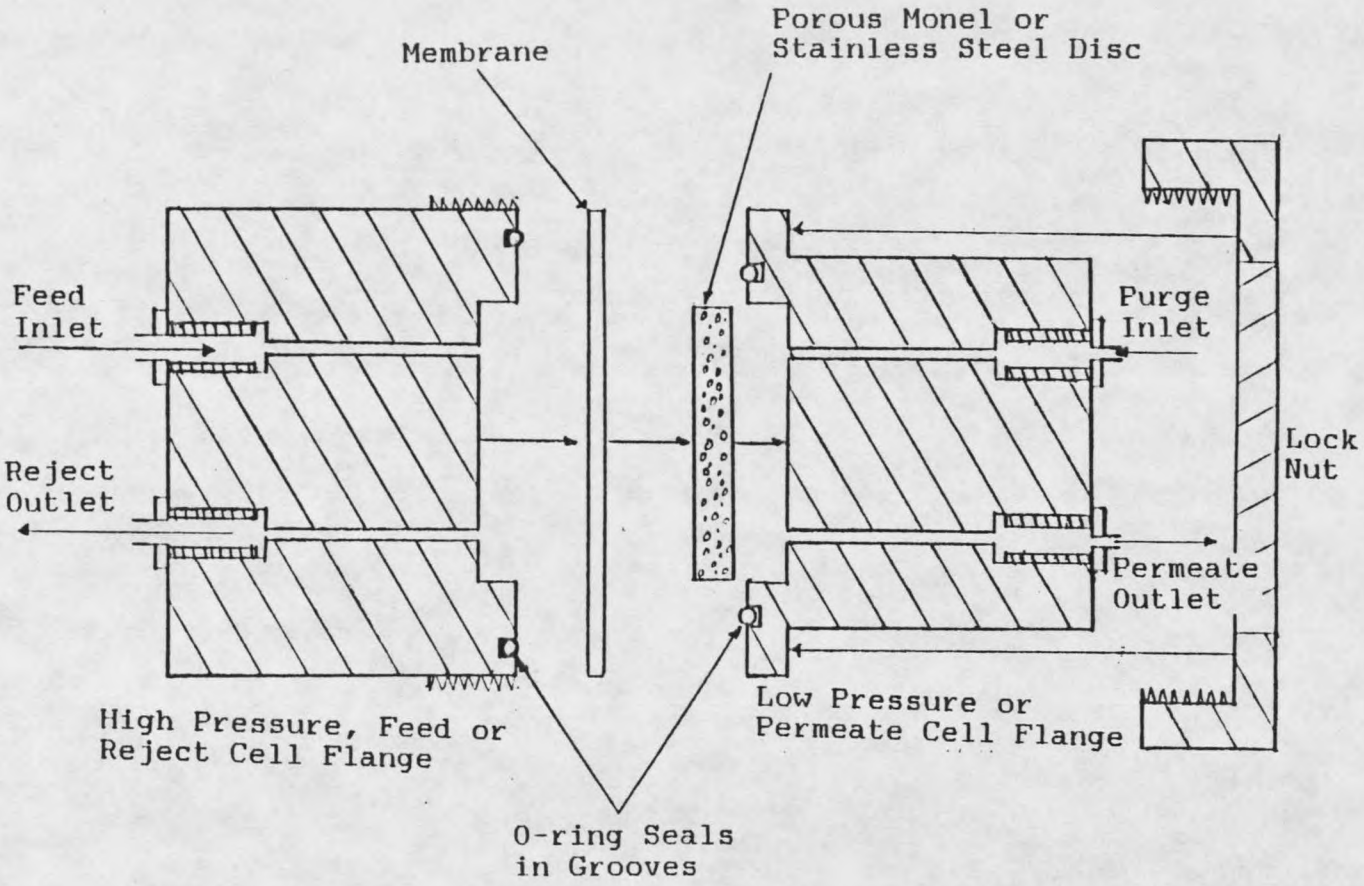

Figure 3. Exploded view of the permeation cell.

A thin porous teflon filter disc placed between the membrane and the metal support buffers the membrane from surface discontinuities around the support/flange perimeter. This teflon filter helped eliminate membrane failure under high pressure loads. With this arrangement, there is approximately 17 cm^2 of membrane area available for permeation. Two o-rings, one in either half of the cell, are placed in machined grooves to provide the necessary seals from the atmosphere and between the two sides of the membrane. The high pressure half of the cell includes a feed inlet, reject outlet and thermocouple well. The inlet on the low pressure side of the cell was connected to the purge gas system, while the low pressure outlet allowed purge gas or permeate to exit the cell.

Feed Gas Supply and Control

A cylinder of BF_3 gas equipped with a Matheson pressure regulator supplied the pressurized feed to the high pressure side of the membrane. The desired operating pressure on the feed side of the membrane was maintained and controlled by a Grove back pressure regulator. A pressure gauge in the reject line was utilized to monitor the feed side pressure. A coil of excess tubing in the feed supply line was placed in the constant temperature enclosure to help insure constant feed gas temperature. All tubing utilized in the feed gas system was constructed of 0.125 inch O.D. stainless steel. All valves in contact with the high pressure BF_3 feed gas had teflon stem seals.

Sample Reservoirs and Flow Measurement

Two sample capture reservoirs, one for each of the permeate and reject gas samples, were constructed from a 6 inch length of 0.25 inch

O.D. stainless steel tubing. Each length of tubing was valved at either end. These capture reservoirs were connected to the respective permeate or reject streams from the permeation cell. When a sample of one or both streams was required, the valves were closed and a "plug" of sample was captured for transport and analysis.

During experimental runs, the outlets of the sample capture reservoirs were connected to a flow measurement manifold. The manifold allowed measurements of the stream flow rates independently with only one flow meter and insured the two outlet streams were never in contact. Flow of the stream being measured was directed through the flow transducer of a Matheson model 8160 mass flow meter, while the other stream vented to the atmosphere. Transfer lines from the sample reservoirs to the manifold and the manifold vent lines were 0.125 inch O.D. teflon tubing. The teflon tubing was used since there were no high pressure requirements and the flexibility facilitated easy connection.

Constant Temperature Enclosure

The permeation test cell was placed in a constant temperature enclosure equipped with an electrical resistance heater and a circulating fan. This enclosure provided the heat source and temperature control for permeation tests at elevated temperatures. The temperature was controlled by a Powerstat variable transformer connected to the resistance heater. Temperature measurement was effected by a Fluke digital thermometer connected to a thermocouple located in the thermowell of the test cell. With this arrangement, the temperature in the enclosure could be controlled and monitored to within 1°C.

Purge System

The purge gas supply system consisted of a cylinder of ultra high purity (UHP) helium connected to a Matheson pressure regulator. Purge gas to the high pressure side of the cell was fed through a valve into the BF_3 supply line just below the BF_3 regulator (refer to Figure 2). A second line was used to supply purge gas through a needle valve to the permeate side of the membrane. This arrangement allowed the entire experimental system to be purged prior to a permeation testing, thus eliminating air and possible contaminants from the system. Furthermore, either the high or low pressure side of the cell could be purged independently.

Experimental Procedures

Permeation Test Procedure

A properly sized membrane was cut from the material to be tested using a permeation cell flange as a template. The membrane was then loaded and sealed in the test cell. The integrity of the membrane and cell seals was tested by pressurizing the high pressure side of the cell with UHP helium. By monitoring any gas flow from the permeate outlet with a beaker of water, undesirable leaks in the membrane could be detected prior to mounting the cell in the test system. The same procedure could have been effected with the purge gas system of the experimental apparatus, but it was less cumbersome when conducted outside of the fume hood.

The pressure-tested permeation cell was mounted in the constant temperature enclosure and the corresponding supply or exit lines were

connected. With all lines connected and the sample reservoirs in place, the purge gas supply valve to the high pressure side of the cell was opened. The purge gas pressure was maintained at approximately 200 psig on the high pressure side of the membrane using the back pressure regulator. Purge gas flow rate was adjusted with the helium tank regulator by increasing helium pressure to just above the pressure maintained by the back pressure regulator. The needle valve controlling purge gas flow to the permeate side of the cell was opened and used to adjust the purge gas flow rate through the low pressure side of the experimental system. It was necessary to maintain the high pressure on the unsupported side of the membrane while adjusting the purge gas flow, since the membrane could easily be ruptured by a pressure surge from the permeate side of the cell. The system was allowed to purge for 10 to 24 hours prior to commencement of a test run.

After suitably purging the system, the purge gas supply valves were closed and the BF_3 supply valve opened, initiating the permeation test. The system was brought up to the desired temperature and the reject flow rate and high pressure were adjusted. The permeate flow was monitored continuously with the mass flow meter. Reject flow was set by simply watching the gas flow being vented to the atmosphere. The permeate flow rate was manually monitored and recorded until a steady state permeation rate was achieved. In order to facilitate representative samples, the system was allowed to operate for several hours after attaining steady state. The reject flow rate was then monitored and recorded. At that point, the sample capture reservoir valves were closed and the samples were ready for analysis. Due to the complex nature of the mass spectral

analysis procedure, a thorough discussion of this topic is delayed to a subsequent section.

Membrane Fabrication

In order to study isotopic separation by the complex transport mechanism, several membranes were fabricated incorporating BF_3-ether complexes of either anisole or phenetole. In other cases, modified membranes were prepared by adding an ether directly. The BF_3 complexes were prepared by bubbling BF_3 feed gas through the respective ether for several hours. Complex formation was accompanied by a color change from the clear ether to a brown/orange color of the complex. In the case of diphenyl ether, complex formation was not attempted although such a complex is certain to exist. Hence, the diphenyl ether was added directly as a membrane modifier.

The fabricated membranes were prepared by dissolving 4 to 5 grams of polyvinylidene fluoride (PVDF) in 5.7 ml of dimethyl formamide (DMF) per gram of PVDF. A predetermined, weighed amount of the ether or BF_3-ether complex was then added to this solution for a 10% mixture on a dry weight PVDF basis. The mixture was heated at 100°C with constant stirring for several hours to insure complete solution, then covered and allowed to stir for 24 to 48 hours at ambient temperature.

The membrane solution was then poured or cast onto a clean glass plate with raised edges. The height of the edges on the mold controlled the membrane thickness, usually about 0.005 inches (5 mil). Once cast onto the glass, the solution was smoothed with a clean glass rod and placed in an oven at 100°C for about 1 hour. The baking process drove

off the DMF solvent, leaving a solid, uniformly thick membrane which was easily removed from the glass plate.

Mass Spectral Analysis

The development of a reliable mass spectral procedure for determination of boron isotopic ratios in BF_3 samples provided a number of unique challenges. Obstacles such as the systematic isolation and elimination of components constructed from materials which reacted with BF_3 and produced unwanted species had to be considered accordingly. It was necessary to determine a number of optimum instrument operating parameters to insure consistent day-to-day analysis of the boron isotopic ratio in BF_3 samples. Considerations such as the choice of mass spectral signals used for isotopic analysis, corrections to these signals for interfering ions, the effect of memory and the isotopic abundance of boron in the BF_3 feed gas were also taken into account. Obviously, the determination of boron isotopic content was neither a straightforward nor simple measurement. Due to the highly non-routine nature of the isotopic abundance analysis, the following discussion is included for completeness.

The mass spectrometer utilized in all analyses was a VG Scientific MM16F located in the chemistry department at Montana State University. This magnetic sector instrument was operated in electron impact ionization (EI) mode with positive ion detection. A data collection system using a Digital PDP8/A hard drive incorporated the necessary software and interfaces for data collection and processing as well as automation and control of many mass spectrometer functions. Consistent analyses were obtained with an amplifier gain (VG Scientific, FA3) of 10^{-6} amps and

response time of 0.3 milliseconds. The electron trap current was 200 μA and the dark current in the source was adjusted daily prior to any analyses. The scan rate of the magnet, which was computer controlled, was 10 seconds/decade and the scan range was between masses 35 and 200. The instrument was calibrated in the standard manner with polyfluorokerosene (PFK), and ion beam adjustments were performed monthly during calibration checks with this reference material.

One of the first problems encountered in the analysis was the presence of interfering signals due to fluorosilicates (SiF_3^+, SiF_2^+, SiF^+). These compounds were determined to occur as a reaction product between BF_3 and the teflon backed silicon rubber septa used for needle ports in classical gas syringe introduction techniques. To eliminate these interferences, the septa and, hence, the usual gas inlet system to the mass spectrometer, were eliminated. The result was the development and incorporation of a unique sample system for introduction of the gas samples into the mass spectrometer.

The sample introduction system developed for the analysis is shown in Figure 4. In this system, a 15 foot coil of 1/16 inch O.D., fine bore stainless steel tubing was connected in place of the GC column at the inlet to the ionization chamber of the mass spectrometer. This column was intended to function as an alternative "molecular leak" used to slow and disperse sample flow into the instrument such that relatively small quantities of sample flowed continuously into the ionization chamber. As a result, the signal intensity remained constant for extended periods of time. This type of behavior is far more desirable than a signal spike due to rapid sample inlet and depletion.

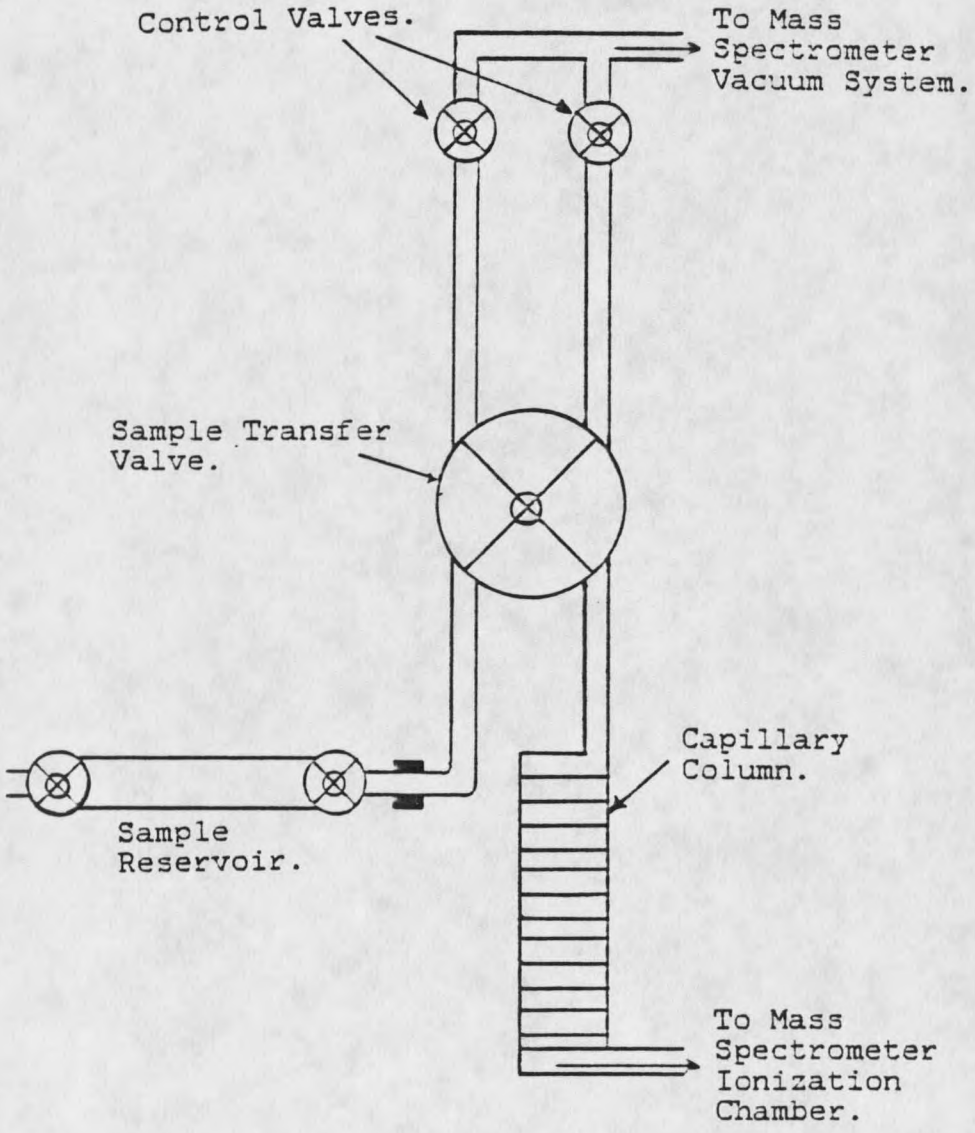

Figure 4. Gas sample introduction system for the mass spectrometer.

The opposite end of the column was connected to a Rheodyne model 7010 sample injection valve. The injection valve divided the gas inlet system into two regions, the sample side and the instrument inlet portion of the system. By utilizing known volume, interchangeable sample loops on this valve, precise and known amounts of sample could be transported from the sample reservoir to the mass spectrometer. The 100 μl volume sample loop used in conjunction with the injection valve was found to provide a sufficient amount of sample over a suitable period of time for consistent analysis. The valved auxiliary vacuum lines provided a means for pumping down the two regions of the inlet system to the operating pressure of the mass spectrometer ($\approx 10^{-7}$ mbar). Thus, sample transport through the inlet system was effected by a pressure difference between the gas sample reservoir and the mass spectrometer.

Sample capture reservoirs were connected to the inlet system by tubing fittings such that these vessels could be easily interchanged. The design allowed the sample side of the valve to be isolated from the mass spectrometer vacuum system, the sample reservoirs interchanged and the system pumped back down to the operating pressure of the instrument. Upon opening the reservoir valve to the gas inlet system, the sample side of the inlet system stabilized at essentially the pressure of the gas sample in the reservoir ($\approx$1 atm).

Using the above described gas inlet system and instrument operating parameters, several injections of a particular sample were introduced to the mass spectrometer. Usually, 100 scans of the sample were averaged per injection. Three or four injections of a sample were analyzed in this manner, with the overall average of % ^{10}B being the accepted value.

Standard deviations were calculated from the results of the individual injections.

The mass spectral signals utilized in all isotopic analyses were those occurring at m/e⁻ 48 and 49, due to the fragment ions $^{10}BF_2^+$ and $^{11}BF_2^+$, respectively. These fragments are the most abundantly formed ionic species during the electron impact ionization process of BF_3. Consequently, the peaks at masses 48 and 49 are the most intense signals in the BF_3 mass spectrum. Use of these signals for the isotopic abundance determination therefore requires a minimum amount of sample. This is beneficial in the reduction of adverse effects caused by high sample pressures and memory in the mass spectrometer.

Denoting signal intensities with square brackets, the ^{10}B mole fraction in a BF_3 sample is calculated from the mass spectral data by:

$$\text{Mole fraction } ^{10}B = \frac{[48]}{[48] + [49]} \qquad (21)$$

Equation (21) is accurate provided the signal intensities, [48] and [49], can be attributed solely to the ions $^{10}BF_2^+$ and $^{11}BF_2^+$, respectively. The relative isotopic abundance can be expressed as a percentage by multiplication of equation (21) by 100%.

Contamination of the m/e⁻ 48 and 49 positions can result from a number of fragment ions formed by ionization of such chemical species as SO_2, SiF_4 and reaction products of water and BF_3. Previous researchers have based the isotopic abundance analysis on the signals at m/e⁻ 10 and 11 due to the fragments $^{10}B^+$ and $^{11}B^+$, respectively [2,3]. Contamination is apparently non-existent at the mass 10 and 11 positions. It became apparent during the course of this study that the $^{10}B^+$ and $^{11}B^+$ ions were

formed in extremely low yield. Consequently, inundation of the mass spectrometer with copious amounts of BF_3 samples would be necessary to provide suitably intense signals at the mass 10 and 11 positions for a meaningful analysis. The use of these signals for analysis was dismissed since the large sample requirements could only serve to aggravate the adverse effects of memory and pressure, as well as cause mechanical problems with the mass spectrometer.

Despite extreme precautions to eliminate contaminant species from the experimental equipment, a number of unexplained signals often showed up in the mass spectra. Typically, varying intensity peaks occurred at m/e^- 47, 66 and 85 in the BF_3 mass spectra. These peaks were the most troubling since they were observed with great frequency. Because the signal intensities at the m/e^- 47, 66 and 85 positions were seldom constant between different samples, the possibility that these contaminants were indigenous to the BF_3 gas cylinder was dismissed. It became apparent that in order to determine if these species were the cause of potential contamination of the m/e^- 48 and 49 signals, their exact nature had to be determined. An accurate mass analysis performed on the peaks at m/e^- 47, 66 and 85 indicated these signals were due to the fragment ions COF^+, COF_2^+ and SiF_3^+, respectively. Hence, silicon tetrafluoride (SiF_4) and carbonyl fluoride (COF_2) were present in the experimental apparatus or being formed in the mass spectrometer.

Silicon tetrafluoride forms the isotopic fragment ions $^{29}SiF^+$ and $^{30}SiF^+$, which can contribute to signals at m/e^- 48 and 49, respectively. The source of this material was never determined, but was occasionally

present in BF_3 samples as witnessed by the appearance of a signal at m/e$^-$ 85 due to the fragment ion $^{28}SiF_3^+$.

Carbonyl fluoride was believed to be a reaction product of BF_3 and CO_2. The presence of COF_2 was witnessed by the appearance of peaks at m/e$^-$ 66 and 47 due to COF_2^+ and COF^+, respectively. Contribution from carbonyl fluoride to the signal at m/e$^-$ 48 was due to the isotopic fragments $^{12}C^{17}OF^+$ and $^{13}C^{16}OF^+$. Contribution to the signal at m/e$^-$ 49 was due to the fragment ions $^{13}C^{17}OF^+$ and $^{12}C^{18}OF^+$. Since the natural abundances of ^{13}C, ^{17}O and ^{18}O are small, contamination of the signals at m/e$^-$ 48 and 49 from carbonyl fluoride is probably negligible.

Repeated efforts and extraordinary precautions were designed to eliminate any interfering materials from the BF_3 samples. Since these attempts failed, corrections were applied to the mass spectral data to remove contaminant contributions to the peaks at m/e$^-$ 48 and 49. These corrections were determined to be negligible, generally changing the isotopic abundance by less than 0.1%. The execution of a meticulously consistent analysis procedure to eliminate day-to-day inconsistencies was found to be much more important than the corrections for consistent analysis results. This implies the day-to-day variations in the analysis were significantly larger than inconsistencies due to contaminant species in the BF_3 samples.

Due primarily to time limitations, an exhaustive study of memory effects was not undertaken. Memory is caused by BF_3 adsorbed on the interior surfaces of the sample inlet system and ion source of the mass spectrometer. When samples of differing isotopic composition are being analyzed, exchange occurs between the adsorbed BF_3 from previous samples

with BF_3 in the current sample. Isotopic ratios in the analyte sample are thus modified by the isotopic composition of previous samples. Intuitively, the memory effect is much more pronounced when samples of widely varying isotopic composition are being analyzed.

Due to the small differences in isotopic composition expected between reject and permeate samples, memory was not considered a significant problem. The inlet system and mass spectrometer were flushed several times with generous amounts of BF_3 analyte over a period of 45 minutes to 1 hour prior to commencement of data acquisition. Following this procedure, memory effects were never noted during analyses. Thus, it appeared that memory was sufficiently reduced and had no adverse effect on isotopic abundance analyses.

The isotopic analysis procedure was developed and evaluated by repeated determinations of the isotopic abundance in the BF_3 feed gas. The results of these analyses, performed with the fully developed procedure, are presented in Table 1. The results of Table 1 represent analyses performed on different days over a period of several weeks. The overall average of 19.477 ± 0.152 % ^{10}B is thought to be a good representation of the isotopic composition in the feed gas. This result conforms well with the reported natural abundance of 19.7% ^{10}B [1]. The slight variation could be due to isotopic fractionation of the boron isotopes occurring in the industrial manufacture of the BF_3. Examination of numerous literature sources has revealed much discrepancy exists concerning the isotopic constitution of many boron compounds. The existence of an "exact" isotopic ratio in naturally occurring boron samples is therefore suspect. The results obtained in Table 1 are well

Table 1. Isotopic abundance of BF_3 feed gas samples.

Sample #	$\bar{x} \pm S_x$ % ^{10}B	Sample size, n*
1	19.328 ± 0.086	4
2	19.387 ± 0.072	3
3	19.400 ± 0.100	7
4	19.649 ± 0.240	4
5	19.520 ± 0.077	7
6	19.533 ± 0.086	6
7	19.389 ± 0.064	4
8	19.535 ± 0.091	6
9	19.752 ± 0.033	4
10	19.599 ± 0.070	5
11	19.441 ± 0.019	3
12	19.193 ± 0.053	4
Overall average	19.477 ± 0.152 % ^{10}B	
Spread = 19.752 - 19.193 = 0.559 % ^{10}B		

*Number of individual BF_3 samples used in calculating the average, $\bar{x}$, and sample standard deviation, S_x.

within the range of compositions that have been reported in the literature.

Initially it was thought that provision of a reasonable and precise isotopic abundance for the BF_3 feed would eliminate the need to analyze reject samples. The permeation experiments were to be conducted in a

manner that the feed and reject compositions would be identical. This is a reasonable approximation if the reject flow rate is maintained substantially higher than the permeate flow, and therefore differences between the feed and reject compositions are undetectable. Thus, only the analysis of permeate samples would be required. Due to large variations in the day-to-day analysis of the feed gas, the thought of this procedure was dismissed. Table 1 indicates variations by as much as 0.556 % ^{10}B are possible between day-to-day analyses. It therefore became obvious that both permeate and reject samples had to be analyzed consecutively to eliminate uncertainties in the calculation of separation factors.

The day-to-day variations in the isotopic abundance of the BF_3 feed gas were attributed to slight daily variations in the calibration, electronics or instrumentation of the mass spectrometer. This conclusion was based on the excellent precision of the individual (daily) analyses. This precision is represented by typical sample standard deviations (S_x) of less than 0.1% for the individual samples.

The differences in isotopic composition between permeate and reject samples were expected to be less than 1.0% ^{10}B. The above discussion and results of the analysis procedure indicate the method appears quite capable of discriminating between the expected isotopic abundances. Based on the maximum sample standard deviation (S_x) of 0.240% ^{10}B for sample number 4, the analysis procedure should be adequate to discern between isotopic compositions differing by as little as 0.25% ^{10}B. In the event smaller differences between reject and permeate samples were exhibited, statistical methods were employed to determine whether or not those differences in isotopic abundance actually existed.

RESULTS AND DISCUSSION

Reactivity Testing

The purpose of the reactivity test was to pre-screen commercial films in an attempt to determine which materials were suitably inert with BF_3 to warrant permeation testing. The need to establish the inertness of the commercial plastics was manifested in a permeation test with a polyvinylfluoride (PVF) film. The PVF membrane was loaded into the permeation cell, checked for integrity, mounted in the experimental apparatus and purged for 24 hours with UHP helium. Upon introduction of the BF_3 to the system, it was discovered that PVF dissolved almost immediately in the feed gas. Consequently, it was desirable to determine the inertness of the commercial plastics with BF_3 prior to permeation testing. Accordingly, the reactivity test was designed and conducted on commercial films scheduled to be tested as membranes.

For the reactivity test, a sample of plastic was placed in a glass container. Air was displaced from the sample container with BF_3 feed gas. The container was sealed and the plastic sample was allowed to stand in the BF_3 environment at ambient temperature and approximately atmospheric pressure. After about 24 hours, the container was opened and the BF_3 allowed to escape. The plastic film was examined and changes in color, physical appearance, texture or other signs of degradation were noted. A PVF sample known to be reactive with BF_3 was included in the reactivity testing as a control sample.

Results of the reactivity testing are presented in Table 2. For convenience, Table 2 is divided into two categories: (a) reactive materials and (b) inert materials. The films in the reactive category were deemed unsuitable as membrane materials. The films in the inert category showed no signs of degradation and appeared suitable for permeation testing. Note that successfully passing the reactivity test offered no conclusive assurances that a plastic would make a suitable membrane material. Degradation could conceivably result at the elevated temperatures and pressures encountered in the permeation cell. Hence, the reactivity tests provided insight concerning those materials which were definitely unacceptable for use as membranes.

Table 2. Results of the reactivity tests.

(a) Reactive Materials

Polymer	Observations
Polyvinyl fluoride	Discolored, dissolves
Polyester	Discolored, brittle
Cellulose acetate	Softened and sticky
Nylon	Softened and sticky
Cellophane	Discolored, sticky

(b) Inert Materials

Teflon
Polyethylene
Polyether sulfone
Polyimide
Polysulfone
Polystyrene
Polypropylene
Saran

Commercial Films

The commercial films successfully passing the reactivity test were subsequently tested to determine if these materials would selectively permeate either of the isotopic constituents of BF_3. The results from the permeation experiments with these commercial membranes are presented in Table 3. Excluded from this tabulated data are polysulfone, polystyrene and saran (polyvinylidene chloride, polyvinyl chloride co-polymer). A polysulfone sample of sufficient size for a membrane was not available for permeation testing. Polystyrene and saran were tested, but proved impermeable to BF_3; therefore, these materials were not included in Table 3.

Except in the case of teflon, the experimental temperatures indicated in Table 3 were necessary to obtain measurable permeation fluxes through the membranes. These temperatures are those at which the corresponding samples were taken for analysis. In all cases, the feed side of the membrane was maintained at 200 psig. The teflon experiments were conducted at temperatures varying between 40°C and 100°C. Reject and permeate samples were taken at several of these temperatures, with the overall analysis results indicated in Table 3.

The separation factors presented in Table 3 are based on ^{10}B selectivity as per equation (15). Thus, $1/\alpha$ represents ^{11}B selectivity as given by equation (20). Recall this nomenclature is mandated by the convention that reported separation factors be greater than unity ($\alpha>1$). A separation factor of unity ($\alpha=1$) therefore indicates no separation of the boron isotopes was observed during permeation testing.

Table 3. Results of BF_3 permeation experiments with commercially available plastics.

Membrane	Experimental Temperature °C	Mole Fraction ^{10}B		Separation Factor
		Permeate	Reject	
Teflon	40-100	0.19533 ± 0.00033	0.19526 ± 0.00029	$\alpha = 1.000$
Polypropylene	96	0.19162 ± 0.00039	0.19233 ± 0.00038	$\alpha = 1.000$
Polyethersulfone	186	0.19889 ± 0.00096	0.19752 ± 0.00033	$\alpha = 1.000$
Polyimide	195	0.19416 ± 0.00079	0.19599 ± 0.00070	$1/\alpha = 1.010$
Polyethylene	89	0.19365 ± 0.00021	0.19441 ± 0.00019	$1/\alpha = 1.005$

The results in Table 3 indicate the permeate and reject compositions were very similar for the individual membranes. It was therefore desirable to eliminate arbitrary or intuitive decisions regarding probable differences between the compositions of the two samples. Thus, an applicable method was required to ascertain if isotopic separation had been observed. Statistical methods were naturally suited to this task. Consequently, statistical inference, or hypothesis testing, was employed to determine whether the reject and permeate compositions were actually different and separation was observed. The separation factors reported in Table 3 reflect the outcome of these statistical methods using a 98% confidence interval. A description and example of the statistical methods employed is presented in Appendix B.

In general, each commercial material was observed to behave differently during the course of the permeation tests. The permeation experiments for the commercial films are discussed individually below.

Teflon

This material was the most extensively tested of the commercial films. It exhibited high permeation rates of BF_3 from ambient temperature to elevated temperatures around 200°C. As expected from theory, the permeation flux increased rapidly with increasing temperature. Teflon was observed to be extremely inert to BF_3 gas over the entire range of experimental temperatures. Isotopic fractionation was never observed, regardless of temperature, in permeation tests with teflon.

Polypropylene

This material was also observed to be very inert to BF_3 gas. It was not extremely permeable to BF_3, but detectable flux was obtained with moderate temperatures. Isotopic separation was not observed with the polypropylene membrane.

Polyethersulfone

Elevated temperatures were required with this material to obtain any permeation flux. PES appeared to react with the BF_3 at the permeation test conditions. Reaction was apparent by a broad range of fragment ions observed in the mass spectral analysis of the permeate sample. The membrane was observed to be very brittle upon removal from the permeation test cell, a further indication of a reaction between PES and BF_3.

Polyimide

This material was observed to be quite impermeable to BF_3 gas until substantial temperatures were achieved. Although the polyimide indicated the greatest degree of selectivity ($1/\alpha = 1.010$) of any tested commercial film, temperature requirements and very low separation make this material impractical for commercial separation schemes. As with PES, polyimide was observed to react slightly with the BF_3 gas. For both polyimide and PES, the demonstrated change in brittleness could be caused by the BF_3 "leaching" out plasticizers or solvents present in these films.

Polyethylene

This material was observed to be inert to BF_3 at the experimental conditions. Detectable permeate flux was observed at moderate

temperatures indicated in Table 3. Although slight ^{11}B selectivity was calculated statistically ($1/\alpha = 1.005$), this result is somewhat suspect by comparison with polypropylene and teflon membrane results. The separation factor is extremely low; hence, this material is an unlikely candidate for commercial separation schemes.

Polystyrene and saran

During permeation experiments with both of these materials, the membranes ruptured due to thermal degradation prior to detecting any BF_3 permeate. The thermal breakdown of the polystyrene membrane occurred at 107°C, while the saran film failed at 134°C. The BF_3 feed gas pressure was maintained at 200 psig on the high pressure side of both membranes. Both plastics are highly "oriented" or cross-linked polymers, and are thus designed to be extremely impervious to gases. Such materials show an exceptional degree of shrinkage with elevated temperatures. The exhibited impermeability of these materials toward BF_3 was thus expected. Membrane rupture was attributed to the film actually pulling apart due to shrinkage at elevated temperatures.

The results obtained from permeation experiments with commercial films discourages the isotopic separation of boron with these materials. This result is hardly surprising based on the sorption/diffusion theory of permeation and the similarity of the boron isotopes. The permeation technique studied with the commercial films requires differences in solubility and diffusivity to effect a separation. As expected for isotopes in general, and for the boron isotopes in particular, the differences in the necessary physical properties are non-existent or

minute at best. Thus, it is apparent that a third parameter, such as differences in chemical properties of the isotopes, must be exploited to effect a reasonable separation during the permeation process.

Fabricated Membranes

A number of preliminary studies were conducted with polyvinylidene fluoride (PVDF) membranes prepared in this laboratory. These fabricated films incorporated phenyl ethers as additives to study the plausibility of complex transport. Prior to presenting these results, a discussion of the problems encountered with these membranes is warranted.

After expending a great deal of time and energy in preparation, permeation testing and sample composition analysis, it was determined that the PVDF membranes were reacting and decomposing in the presence of BF_3 at the experimental temperatures and pressures. The BF_3 reaction was determined to be indigenous to the PVDF or solvent system (DMF) used in membrane preparation. Both the unmodified or blank films and the ether containing membranes became discolored and very brittle during permeation experiments. Consequently, a fabricated membrane survived, at best, for a single permeation experiment.

Further signs of decomposition were observed in the mass spectra of permeate samples obtained in all experiments. Huge quantities of undeterminable fragment ions, generally the same ones, were observed in permeate mass spectra. With all but a few exceptions, permeate analysis was impossible due to low signal intensity of the masses of interest.

Despite these problems, a few encouraging separation results were obtained. These results are tabulated in Table 4. All tabulated results

Table 4. Results of permeation experiments with fabricated membranes.

Membrane Modifier	Mole Fraction ^{10}B		Separation Factor
	Permeate	Reject	
10% BF_3 - Phenetole	0.20975 ± 0.00950	0.19582 ± 0.00703	1.090
" "	0.22974 ± 0.01164	0.19515 ± 0.00121	1.230
10% BF_3 - Anisole	0.20566	0.19442	1.073
" "	0.19763	0.19328 ± 0.00086	1.028
10% Diphenyl ether	0.19751 ± 0.00043	0.19393 ± 0.00109	1.023

were obtained at 120°C and with a feed pressure of 200 psig on the high pressure side of the membranes.

Each of the membranes in Table 4 exhibited ^{10}B selectivity, reflected in the listed separation factors. Due to membrane degradation, composition data was often too limited for appropriate statistical treatment. The ^{10}B mole fractions and thus the tabulated separation factors were not submitted to statistical evaluations.

Despite the inability to interpret these results statistically, the separation factors reported in Table 4 indicate that some degree of isotopic fractionation had indeed occurred. The separation factor of $\alpha = 1.230$ obtained with the second 10% BF_3•phenetole membrane is quite large compared with the other separation factors listed in Table 4; this result is therefore suspect. Nevertheless, these results indicate a substantial increase in selectivities over those observed with the commercially available polymers, strengthening the case for complex transport mechanisms and membranes as a possible means of isotopic enrichment.

The trend exhibited in separation factor versus membrane additive is also important. Note that the phenetole complex containing membrane provided the largest separation factor, the 10% BF_3•anisole membrane is in the middle, and the diphenyl ether film provides the lowest degree of separation. Previous researchers have reported single stage isotopic equilibrium constants of 1.039 for the phenetole complex and 1.0291 for the anisole complex in the isotope exchange reaction given by equation (19) [2, p. 13]. The exhibited trend in separation factor versus the phenetole and anisole additives is consistent with these previous

thermodynamic studies. Thus, this trend conforms well to theory and adds credibility to further study of complex transport as a viable method for the separation of boron isotopes.

It was obvious in the complex transport permeation tests that PVDF was an unsuitable support material for the phenyl ether modifiers. Some of the decomposition problems may have resulted from the dimethyl formamide (DMF) used as a solvent for the PVDF. Residual amounts of solvent certainly remain entrained in the membrane during the fabrication process. Other suitable PVDF solvents, such as dimethyl sulfoxide, were not tested.

Another foreseeable concern pertains to the decomposition of the BF_3-phenylether complexes. The complexes are reported to decompose readily with elevated temperatures [2, 3]. The effect decomposition would have on separation was not studied; however, it appears that membrane degradation was not due to complex decomposition since unmodified films behaved in the same manner as ether containing membranes. It would be necessary and interesting to study the effects of complex decomposition on separation factor provided a suitably inert support material should be developed.

CONCLUSIONS

(1) The commercial films studied in this research were impractical for use as membranes in boron isotope separation schemes.

(2) Of the commercial films tested, teflon was the most inert and permeable membrane for BF_3 gas. However, teflon was not selective in permeation of boron isotopes.

(3) The conformity of complex transport separation trends with theoretical predictions indicates these membranes are the most promising of the films studied in this research.

(4) Polyvinylidene fluoride or residual dimethyl formamide solvent in the fabricated membranes is reactive with BF_3 gas. Hence, the PVDF membranes fabricated for this research provide an inappropriate support matrix for the complex transport carriers.

(5) Complex transport results with the fabricated membranes indicate an enhanced degree of selectivity over that obtained with commercial films.

RECOMMENDATIONS FOR FURTHER STUDY

(1) Further permeation testing with commercially available membranes should be limited to those films containing chemical species and linkages thought to be conducive to complex transport mechanisms.

(2) Further research involving complex transport mechanisms is recommended. Development or determination of inert support materials which incorporate the carrier additives should be targeted in future studies. Accomplishing this goal would provide an excellent method for the study and evaluation of chemical systems applicable to boron isotope separation.

REFERENCES CITED

1. Dean, J.A., editor, Lange's Handbook of Chemistry and Physics, 13th Edition, McGraw-Hill, New York, 1985, p. 3-17.

2. Palko, A.A., "The Chemical Separation of Boron Isotopes," ORNL #5418, Oak Ridge National Laboratory Chemistry Division, Oak Ridge, Tenn., June 1978.

3. Murphy, G.M., editor, "Separation of Boron Isotopes," U.S. Atomic Energy Comm., Technical Information Services, Oak Ridge, Tenn. NNES III-5 1952 (Declassified May 1957).

4. Conn, A.L. and Wolf, J.E., Ind. Eng. Chem. 50, 1231, Sept. 1958.

5. Chilton, C.H., Chem. Eng. 64, No. 5, 148 (1957).

6. Paulson, G.T., Manager, Criticality Safety, Westinghouse Idaho Nuclear Co., Idaho Falls, ID, Personal Communication, June 1988.

7. Matson, S.L., Chem. Eng. Sci. 38, No. 4, 1983.

8. Green, D., editor, Perry's Chemical Engineers Handbook, 6th Edition, McGraw-Hill, New York, 1984, p. 3-256.

9. Meares, P., editor, Membrane Science Processes, Elsevier Scientific, New York, 1976, p. 10.

10. Hwang, S.T. and Kammermeyer, K., Membranes in Separations, John Wiley & Sons, New York, 1975.

11. Baker, R.W. and Blume, I., Chemtech, April 1986.

12. Johnson, R., Elementary Statistics, 2nd Edition, Duxbury Press, Massachusetts, 1976.

13. Juran, J.M. and Gryna, F.M., Quality Planning and Analysis, McGraw-Hill, New York, 1980.

APPENDICES

APPENDIX A

Table of Nomenclature

A	Membrane surface area perpendicular to flux direction.
C_A	Concentration of component A.
C_{Ah}	Concentration of component A on the high pressure or reject side of the membrane.
C_{Al}	Concentration of component A on the permeate side of membrane.
D	Diffusivity coefficient.
D_o	Standard state diffusivity coefficient.
E_D	Energy of diffusion.
ΔH_s	Heat of solution.
L	Molar flow rate of permeate stream.
N_A	Permeation flux of component A.
p_h	Total pressure on reject or feed side of membrane.
p_l	Total pressure on permeate side of membrane.
p_r	Pressure ratio $\equiv p_l/p_h$
P_A^*	Permeability coefficient of component A.
P_B^*	Permeability coefficient of component B.
P_A^m	Molar permeability of component A.
P_B^m	Molar permeability of component B.
R	Universal gas constant.
S	Solubility coefficient $\equiv$ Henry's law constant.
S_o	Standard state solubility coefficient.
T	Absolute temperature
x_A	Mole fraction of component A in reject.
y_A	Mole fraction of component A in permeate.
z	Direction coordinate.

Greek Letters

α Overall separation factor.

α^* Ideal separation factor.

δ Membrane thickness.

APPENDIX B

Statistical Methods

The statistical calculations and methods employed here follow standard procedures found in many statistics textbooks [12,13].

The sample mean, $\bar{x}$, and sample standard deviation, S_x, are calculated according to the following equations:

$$\bar{x} = \frac{\Sigma x_i}{n}$$

$$S_x = \pm \left(\frac{\Sigma (\bar{x} - x_i)^2}{n - 1} \right)^{1/2}$$

where x_i represents the value of the individual data points and n represents the sample size or number of observed data points.

Hypothesis testing is a method of statistical decision making or inference. The null hypothesis, H_o, is generally a statement that a population parameter ($\bar{x}$, S_x, etc.) has a specific value. The alternative hypothesis (H_a) is a statement that the population parameter has a different value than specified in the null hypothesis. Once these hypotheses are formed, the null hypothesis is assumed to be a true statement until proven otherwise.

The next step involves determining the appropriate test statistic, specifying a level of significance, μ, or confidence level ($1-\mu$) and determining the critical region. The critical region is the set of values of a test statistic that will cause rejection of the null hypothesis. That is to say, a value of the test statistic inside the critical region will be sufficient evidence to accept H_o, and for test statistic values outside the critical region, H_o will be rejected. Only type I errors are dealt with in this discussion.

It is easiest to present this method by example. Thus, consider the following data obtained from permeation experiments with polypropylene:

% ^{10}B in permeate	% ^{10}B in reject
19.095	19.178
19.159	19.259
19.193	19.260
19.186	19.236
19.175	
$\bar{x}_p = 19.162$	$\bar{x}_r = 19.233$
$s_p = \pm 0.039$	$s_r = \pm 0.038$
$n_p = 5$	$n_r = 4$

It is desired to determine if $\bar{x}_p = \bar{x}_r$ (no separation) or $\bar{x}_p \neq \bar{x}_r$ (isotopic separation). In order to answer this question, the proper test statistic and method depends on which of the following cases is applicable to the data:

$$\text{Case 1: } \sigma_p^2 = \sigma_r^2 \quad \text{or} \quad \text{Case 2: } \sigma_p^2 \neq \sigma_r^2$$

where σ represents the standard deviation of the population. Since σ is unknown, S (sample standard deviation) is used as a viable estimate of σ. Thus, the following hypothesis test is employed to determine which case exists:

$$H_o : S_p^2 = S_r^2 \quad \text{(Case 1)}$$

$$H_a : S_p^2 \neq S_r^2 \quad \text{(Case 2)}$$

A confidence level of 98% is chosen, hence:

$$1 - \mu = 0.98 \qquad \mu = 0.02 \qquad \mu/2 = 0.01$$

The critical region is determined from standard F distribution tables with $\mu = 0.1$ [12, p. A40]:

$$F(n_p\text{-}1,\ n_r\text{-}1,\ \mu/2) = F(4,3,0.01) = 28.7$$

$$F(4,3,0.99) = [F(3,4,0.01)]^{-1} = [16.7]^{-1} = 0.0599$$

Defining and calculating the test statistic, F*, as:

$$F^* \equiv \frac{S_p^2}{S_r^2} = \frac{0.039^2}{0.038^2} = 1.05$$

The test statistic F* is inside the critical region ($0.0599<F^*<28.7$) and the null hypothesis is accepted. Hence, the data conforms to case 1 ($\sigma_p^2 = \sigma_r^2$). In fact, all experimental data obtained in permeation testing obeyed case 1 criteria. With this knowledge, the initial question ($\bar{x}_p \stackrel{?}{=} \bar{x}_r$) can be answered by hypothesis testing.

Thus, the null hypothesis and alternative hypothesis are first formed:

$$H_o : \bar{x}_p = \bar{x}_r \qquad H_a : \bar{x}_p \neq \bar{x}_r$$

The critical or acceptance region is established from standard t tables for $\mu/2 = 0.01$ [12, p. A33]:

$$t\ (n_p + n_r - 2,\ \mu/2) = t\ (7,0.01) = \pm 3.00$$

The pooled standard deviation, s_p, is calculated:

$$S_p = \left\{ \frac{(n_p-1)S_p^2 + (n_r-1)S_r^2}{n_p + n_r - 2} \right\}^{\frac{1}{2}} = \left\{ \frac{(4)(0.039)^2 + (3)(0.038)^2}{7} \right\}^{\frac{1}{2}} = 0.0386$$

The test statistic is determined:

$$t^* = \frac{\bar{x}_p - \bar{x}_r}{s_p(1/n_p+1/n_r)^{\frac{1}{2}}} = \frac{(19.162 - 19.233)}{0.0386\ (1/5+1/4)^{\frac{1}{2}}} = -2.744$$

Because the test statistic is inside the acceptance region ($-3.00<t^*<3.00$), the null hypothesis is not rejected, and the two samples are statistically the same. Hence, with a confidence level of 98%, no separation occurred with the polypropylene membrane.